厚生労働科学研究費補助金（化学物質リスク研究事業）
分担研究報告書

化学物質の代謝活性化の予測モデルに関する研究
分担研究者　山添　康　東北大学大学院薬学研究科　薬物動態学分野教授

研究要旨　化学物質の安全性を評価するために、化学物質の代謝部位と関与酵素の予測が必要とされる。化学物質の遺伝毒性、癌原性、臓器障害等に関与する CYP1A2 酵素の基質特異性に基づく代謝の予測を試み、酵素 3D モデルがなくても発現系 CYP1A2 による代謝データから条件を導くことで予測が可能なことが明らかになった。

A. 研究目的

　生体内での代謝変換の知見は、化学物質の安全性評価のための重要な情報である。ヒト環境中には多数の化学物質が含まれ、毎日多くの化学物質に我々は接触しており、また食事成分として意図的および非意図的に取り込んでいる。これら多数の化学物質の安全性を、従来手法で短期間に評価することは難しく、たとえ出来てとしてもコストが膨大な額になる。現在添加物香料のような微量物質について簡略化のルール作りが進められている。現在このルールにも代謝経路の有無についての項目があり、安全性評価の指標の1つとなっている。

　過去10年間に医薬品を中心に代謝に関する情報の流れに大きな変化があった。従来実験動物で得られた代謝情報をヒトに外挿して代謝が評価されていた。しかし代謝酵素の研究が進展してヒトと実験動物の種差が明瞭になり、ヒトにおける代謝はヒト由来の試料を用いて評価することが前提となった。同様の種差は医薬品だけでなく多くの化学物質にも当てはまる。この問題を乗り越えるためヒト酵素発現系で得られた代謝情報をデータベース化して、これを基に単一酵素ごとに基質特異性を明らかにして、この情報から未評価化学物質の代謝特性を予測する系を開発することを試みた。

　化学物質の安全性評価において癌原性や遺伝毒性は化学物質の構造と代謝に深く関わっている。本研究ではこれら試験に深く関わるチトクローム P450 の CYP1A2 を取り上げ、解析した。

B. 研究方法
　化学物質の代謝情報

　ヒト CYP1A2 の発現系試料を用いて測定された代謝データを収集した。ヒト CYP1A2 の発現系には酵母細胞、昆虫細胞など宿主には違いがあり、補酵素からの電子伝達する NADPH-cyt P450 還元酵素の発現レベルにも差がみられる。しかしながら今回のデータ収集ではこれらを区別せず、基質特性情報として得られたものをリストした。

　化学物質の代謝についての情報精度にもかなりの違いが見られる。主代謝物のみを測定対象としたデータと副生成物を含めた定量データを含む論文もあったが、今回は必要事項の抜き出しに必要な項目のみを採用した。

　データの収集は Medline を用い、PubMed 検索で該当する文献を選択した。

　検索項目は、基本的に CYP1A, human liver としたが、化合物によっては該当する論文が選択されないため、阻害薬物等の情報を付加して収集した。

C. 研究結果

得られた化学物質情報を下に示す。

Substrate	Product	CYP form1
7,8-Dihydroxy-7,8-dihydrobenzo[a]pyrene	9,10-oxide	CYP1A1
3-Methylcholanthrene		CYP1A
Almotriptan		CYP3A4
Atrazine	iPr-OH	CYP1A2
Benzo[a]pyrene	3-hydroxylation	CYP1A
Benzo[a]pyrene	7,8-oxide	CYP1A
Benzo[a]pyrene	6-OH	CYP1A
Benzo[c]phenanthrene		CYP1A2
Clozapine		CYP1A2
Coumarin	coumarin 3,4-epoxide	CYP1A1/2
Cyclobenzaprine	N-demethylation	CYP1A2
Daidzein		CYP1A2
DMXAA	6-methylhydroxylation	CYP1A2
Fluvoxamine		CYP1A2
Furafylline	inf mechanism	CYP1A2
Imipramine		CYP1A2
JANEX-1	O-demethylation	CYP1A2
Lidocaine	N-DE	CYP1A2
Lisofylline	pentoxyfylline	CYP1A2
PhIP	N-OH	CYP1A2
Primaquine		CYP1A2
Promazine	5-sulphoxidation	1A1>2B6>1A2
Promazine	N-demethylation	2C19>2B6>1A1>1A2
Ropivacaine	3-OH-ropivacaine	CYP1A2
Ropivacaine	4-OH-ropivacaine	CYP3A4
Ropivacaine	2-OH-methyl-ropivacaine	CYP3A4
Ropivacaine	2',6'-pipecoloxylidide	CYP3A4
Rutaecarpine	inh	CYP1A2
S 16020	Unknown	CYP1A2
Sanguinarine	inh mechanism	CYP1A2
Tacrine	7-OH	CYP1A2

Tanshinone IIA	inf	CYP1A2
Terbinafine	DHDiol	CYP1A2
Terbinafine	N-DM	CYP1A2
Thalidomide	5,5'-OHs	CYP1A
Theophylline	demethylation	CYP1A2
Theophylline	hydroxylation	CYP1A2
Tizanidine	ring Ox	CYP1A2
Verlukast	epoxidation	CYP1A1
Zaleplon	N-DE	CYP3A4
Zolmitriptan	N-demethylation	CYP1A2
Zolpidem	alcohol deriv	CYP1A2

ここで CYPform1 は主代謝酵素として報告されている分子種で、化学物質によっては CYP1A2 が主酵素でなく、むしろ副次的に関与する場合リストには他の分子種のみが記載されているものがある。代表的な化学物質と CYP1A2 による酸化部位を別紙に示した。

予測に当たっての基本的考え方

チトクローム P450 の酸化反応は、基質の一部が酵素の特定部位に接触して捕捉されることではじまる。ついで、ヘム近傍の環境に合うコンフォメーションを採ったときに酵素内に固定され酸化を受ける。

最初に接触する部位を trigger site と呼ぶ。他の P450 分子種では基質構造内に基質の構造を酸化部位とオープン空間にはいる部位に分ける pinching point と呼ぶ箇所がある。CYP1A2 では trigger site が平板状でその直線上に pinching point があると予測されるため、pinching point の決定は不必要となる。代表的な約10種の物質についてこの原則を適用して酸化部位と trigger site の関係を調べた結果、酸化部位は特定範囲の距離を中心に分布することが明らかとなった。この距離はベンゼン環3個分に相当する。

この段階で、trigger pinching oxidizing 各部位の同一平面性が必要な要素であることが判明したので、これらを統一的に扱うルールとして pyrene rule を考案した。

Pyrene rule について

下図の pyrene は4環性の平面分子である。ここで CYP1A2 に基質は赤字矢印の部位が trigger site に捕捉されると考える。平面性が重要な要素である。空間上下左右の構造が一定の条件を満たすと、緑矢印の酸化部位がヘム近傍に向かって配位して固定されると考える。これら2部位の間をさらに固定する必要があり、上下環いずれかのの炭素が pinching point を兼ねる。
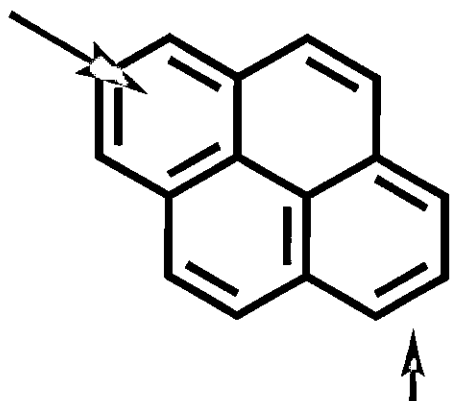
このように考えると、被検化合物を pyrene と重ねることによって適合性を調べることが可能となる。
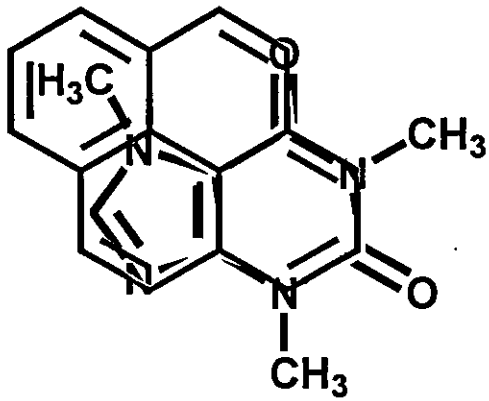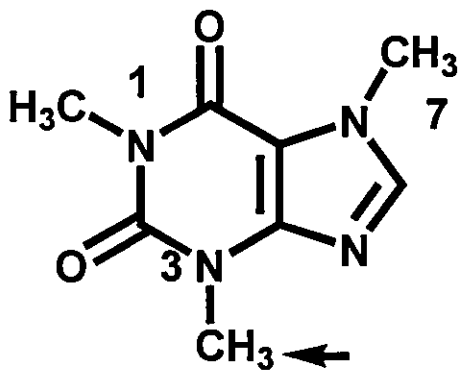
基本的には3環にわたって重なる部位の多い物質ほど、適合性があると考える、

ヘムは緑の矢印下方から接近するので側鎖がこの下方2炭素までの範囲にあれば基質となる。

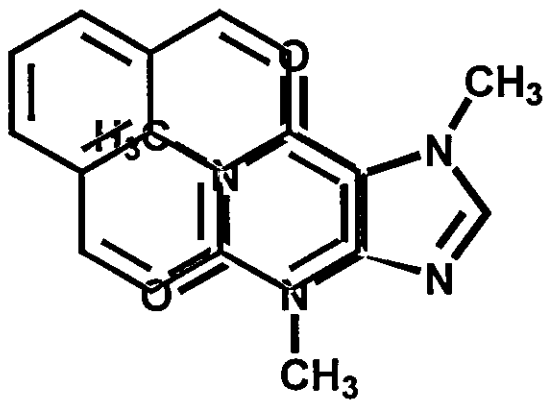酸化部位はベンゼン環1個分の余裕があり、下方の naphthalene は anthracene になっても収容可能である。左下に pyrene 下端を超えて伸張はできない。

また酸化部位の上も naphthalene 環の高さまで可能である。

Trigger 部位の上は比較的余裕がある。

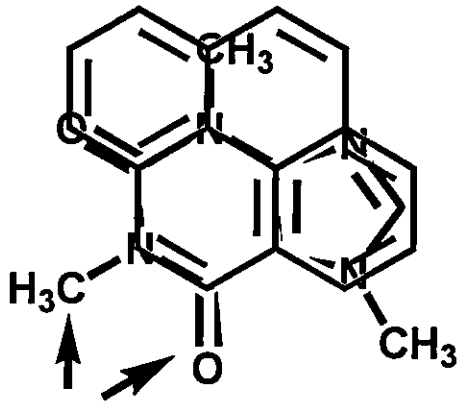Caffeine の場合

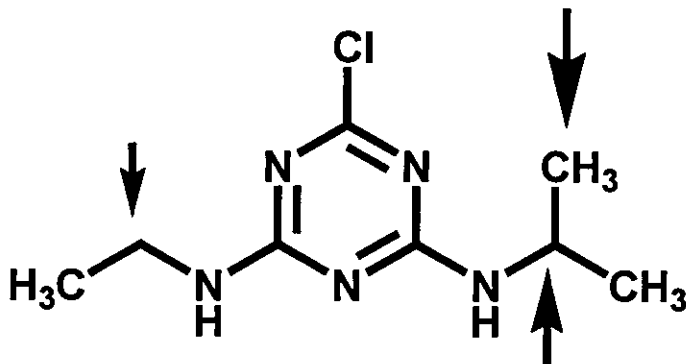N3—methyl 基の酸化が優先する。　N—7methyl 基が何とか trigger site の広さをカバーしている。

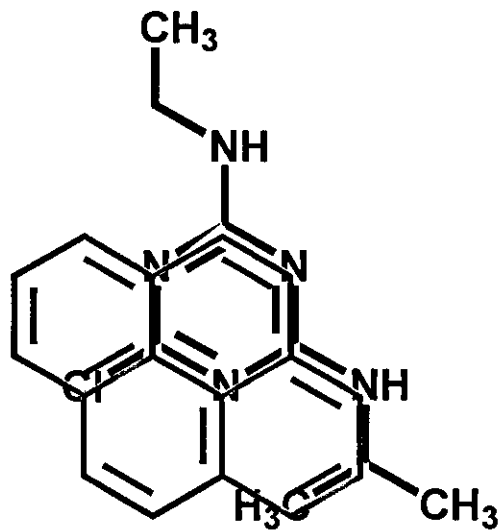この配置では trigger site の平面を保持できないと考えられる。また5員環上のメチルが邪魔となる。

hinder ?

N-7-methyl 基の酸化は左下に来る N-3-methyl/carbonyl 基の障害を受ける。結果的に N-3-methyl 基の酸化が優先すると判断する。

Atrazine の酸化代謝

Atrazine

矢印の部位が CYP1A2 によって代謝される。

イソプロピル基もエチル基も Pyrene 則に当てはまり、代謝されやすいと考えられる。クロル原子があることによって trigger されやすい構造になっていると考えられる。
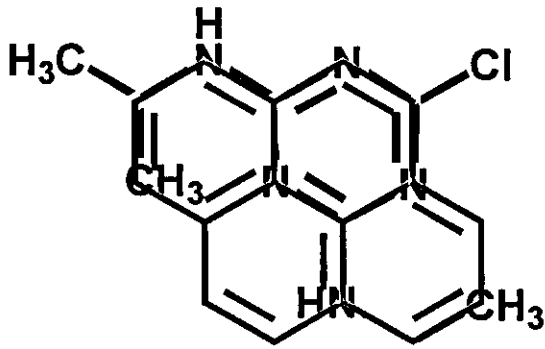
　上図のようにクロル原子が関与しないで pyrene 則に当てはめることも可能で特にエチル基が酸化される場合には適合は位置となる。

D. 考察

　CYP1A2 の基質となる化学物質はいずれも平面平板状の配置が可能な物質であることが明らかとなった。多くの場合平面構造から予想が可能であるが、ねじれ等の要因を知るため3次元構造として評価する必要性が明らかとなった。

E. 結論

　表に示した化学物質の代謝部位と pyrene 則の適用性比較から trigger 部位の奥行き等の確度を向上させる必要があるが、予測が可能なことが明らかとなった。

F. 健康危険情報

　特になし

Ⅲ．研究成果の刊行に関する一覧表

書籍

著者名	論文タイトル	書籍全体の編集者名	書籍名	出版社名	出版地	出版年	ページ

雑誌

著者名	論文タイトル	発表誌名	巻名	ページ	出版年
Homa, M., Izumi M., Sakurada Y., Tadokoro S., Sakamoto H., Wang W., Yatgai F. and Hayashi M	Deletion, rearrangement, and gene conversion; genetic consequences of chromosomal double-strand breaks in human cells	Environ. Mol. Mutagen	42	288-298	2003
Itoh, T., Kuwahara T., Suzuki T., Hayashi M.and Ohnishi Y	Regional mutagenicity of heterocyclic amines in the intestine: mutation analysis of the *cII* gene in lambda/*lacZ* transgenic mice	Mutat. Res.	539	99-108	2003
Yamada, K., Suzuki T., Kohara A., Hayashi M., Mizutani T. and Saeki K	In vivo mutagenicity of benzo[*f*]quinoline, benzo[*h*]quinoline, and 1,7-phenanthroline using the *lacZ* transgenic mice	Mutat. Res.	559	83-95	2004
Zang, Li, Sakamoto H., Sakuraba M., D-S Wu, L-S Zhang, Suzuki T., Hayashi M. and Honma M.	Genotoxicity of microcystin-LR in Human lymphoblastoid TK6 cells.	Mutat. Res.	557	1-6.	2004
Suzuki, H., Shirotori T., and Hayashi M.	A liver micronucleus assay using; young rats exposed to diethylnitrosamine: methodological establishment and evaluation	Cytogenet. Genome. Res.	104	299-303	2004
林真，長尾美奈子，祖父尼俊雄，森田健，能美健彦，本間正充，宇野芳文，葛西宏，佐々木有，太田敏博，田中憲穂，中嶋圓，布柴達夫	食品および食品添加物に関する遺伝毒性の検出・評価・解釈に関する臨時委員会の活動中間報告	Eviron. Mutagen Res.	26	275-283	2004
Ema M, Harazono A, Hirose A and Kamata E	Protective effects of progesterone on implantation failure induced by dibutyltin dichloride in rats	Toxicol Lett.	143	233-238	2003
Koizumi M, Noda A, Ito Y, Furukawa M, Fujii S, Kamata E, Ema M and Hasegawa R.	Higher susceptibility of newborn than young rats to 3-methylphenol	J Toxicol Sci.	28	59-70	2003
Ema M, Miyawaki E, Hirose A and Kamata E.	Decreased anogenital distance and increased incidence of undescended testes in fetuses of rats given monobenzyl phthalate, a major metabolite of butyl benzyl phthalate	Reprod Toxicol.	17	407-412	2003

著者名	論文タイトル	発表誌名	巻名	ページ	出版年
広瀬明彦、江馬 眞、鎌田栄一、小泉睦子、長谷川隆一	ビスフェノール A の内分泌かく乱作用のヒトへの影響評価	日本食品化学会誌	10	1-12	2003
Fukuda, N., Ito, Y., Yamaguchi, M., Mitsumori, K., Koizumi, M., Hasegawa, R., Kamata, E. and Ema, M	Unexpected nephrotoxicity induced by tetrabromobisphenol A in newborn rats	Toxicol. Lett.	150	145-150	2004
Takahashi M., Ogata H., Izumi H., Yamashita K., Takechi M., Hirata-Koizumi M., Kamata E., Hasegawa R. and Ema M	Comparative toxicity study of 2,4,6-trinitrophenol (picric acid) in newborn and young rats	Cong Anom.	44	204-214	2004
Hirose A., Hasegawa R., Nishikawa A., Takahashi M. and Ema M.	Revision and establishment of Japanese drinking water quality guidelines for di(2-ethylhexyl) phthalate, toluene and vinyl chloride-Differences from the latest WHO guideline drafts-	J Toxicol Sci.	29	535-539	2004
高橋美加、平田睦子、松本真理子、広瀬明彦、鎌田栄一、長谷川隆一、江馬 眞	OECD 化学物質対策の動向(第5報)	衛研報告	122	37-42	2004
広瀬明彦, 江馬 眞	生殖発生毒性を指標としたダイオキシンの耐容1日摂取量(TDI)算定の考え方について	衛研報告	122	56-61	2004
Hashimoto A., Amanuma K., Hiyoshi K., Takano H., Masumura K., Nohmi T. and Aoki Y	In Vivo Mutagenesis Induced by Benzo[a]pyrene Instilled Into the Lung of gpt Delta transgenic Mice	Environ. Mol. Mutagen.	45	In press	2005
松本理, 丸山若重, 広野靖史郎, 青木康展, 松本幸雄, 中杉修身	大気中の化学物質の複合曝露による発がんリスクの評価	日本リスク研究学会誌	15	55-67	2004
Maruyama W., Yoshida K. and Aoki T	Dioxin Health Risk to Infants Using Simulated Tissue Concentrations	Environ. Toxicol. Pharmacol.	18	21-37	2004
青木康展	これからの環境モニタリングとバイオアッセイ	環境と測定技術	32	26-32	2005
Takahashi YK., Kurosaki M., Hirono S. and Mori K	Topographic representation of odorant molecular features in the rat olfactory bulb	J. Neurophysiol.	92	2413-2427	2004
Tsuchida K., Hisaaki C., Takakura T., Yokotani J., Aikawa Y., Shiozawa S., Gouda H. and Hirono S	Design, Synthesis, and Biological Evaluation of New Cyclic Disulfide Decapeptides That Inhibit the Binding of AP-1 to DNA	J.Med.Chem	47	4239-4246	2004

著者名	論文タイトル	発表誌名	巻名	ページ	出版年
Nagata T., Motoyama T., Hirono S. and Yamaguchia I.	Identification, characterization, and site directed mutagenesis of recombinant pentachlorophenol 4-monooxygenase	Biochim. Biophys. Acta.	1700	151-159	2004
Oda A., Yamaotsu N. and Hirono S.	Studies of Binding Modes of (S)-Mephenytoin to Wild Types and Mutants of Cytochrome P450 2C19 and 2C9 using Homology Modeling and Computational Docking	*Pharm. Res.*	21	2270-2278	2004
Nagata Y., Kusuhara H., Hirono S., Endou H. and Sugiyama Y	CARRIER-MEDIATED UPTAKE OF H2-RECEPTOR ANTAGONISTS BY THE RAT CHOROID PLEXUS: INVOLVEMENT OF RAT ORGANIC ANION TRANSPORTER 3	*Drug Metab. Dispos.*	32	1040-1047	2004
Hirono S., Nakagome I., Imai R., Maeda K., Kusuhara H. and Sugiyama Y.	Estimation of the Three-Dimensional Pharmacophore of Ligands for Rat Multidrug- Resistance-Associated Protein 2 using Ligand-Based Drug Design Techniques	*Pharm. Res.*	22	260-269	2005 In press
Matsubara T., Kim H. J., Miyata M., Shimada M., Nagata K. and Yamazoe Y	Isolation and characterization of a new major interestinal CYP3A form, CYP3A62, in the rat	J. Pharmacol. Exp. Ther.	309	1282-1290	2004
Miyata M., Tozawa A., Otsuka H., Nakamura T., Nagata K., Gonzalez F. J and Yamazoe Y.	Role of farnesoid X receptor in the enhancement of canalicular bile acid output and excretion of unconjugated bile acids: a mechanism for protection against cholic acid-induced liver toxicity	J. Pharmacol. Exp. Ther.	312	759-766	2005

8

IV．研究成果の刊行物・別冊

Deletion, Rearrangement, and Gene Conversion; Genetic Consequences of Chromosomal Double-Strand Breaks in Human Cells

Masamitsu Honma,[1]* Masako Izumi,[2] Mayumi Sakuraba,[1]
Satoshi Todokoro,[1] Hiroko Sakamoto,[1] Wensheng Wang,[1] Fumio Yatagai,[2]
and Makoto Hayashi[1]

[1]*Division of Genetics and Mutagenesis, National Institute of Health Sciences,
Setagaya, Tokyo*
[2]*Division of Radioisotope Technology, Institute of Physical and Chemical Research,
Wako, Saitama, Japan*

Chromosomal double-strand breaks (DSBs) in mammalian cells are usually repaired through either of two pathways: end-joining (EJ) or homologous recombination (HR). To clarify the relative contribution of each pathway and the ensuing genetic changes, we developed a system to trace the fate of DSBs that occur in an endogenous single-copy human gene. Lymphoblastoid cell lines TSCE5 and TSCER2 are heterozygous (+/−) or compound heterozygous (−/−), respectively, for the thymidine kinase gene (TK), and we introduced an I-SceI endonuclease site into the gene. EJ for a DSB at the I-SceI site results in TK-deficient mutants in TSCE5 cells, while HR between the alleles produces TK-proficient revertants in TSCER2 cells. We found that almost all DSBs were repaired by EJ and that HR rarely contributes to the repair in this sys- tem. EJ contributed to the repair of DSBs 270 times more frequently than HR. Molecular analysis of the TK gene showed that EJ mainly causes small deletions limited to the TK gene. Seventy percent of the small deletion mutants analyzed showed 100- to 4,000-bp deletions with a 0- to 6-bp homology at the joint. Another 30%, however, were accompanied by complicated DNA rearrangements, presumably the result of sister-chromatid fusion. HR, on the other hand, always resulted in non-crossing-over gene conversion without any loss of genetic information. Thus, although HR is important to the maintenance of genomic stability in DNA containing DSBs, almost all chromosomal DSBs in human cells are repaired by EJ. Environ. Mol. Mutagen. 42:288-298, 2003.   © 2003 Wiley-Liss, Inc.

Key words: double-strand breaks; end-joining; inter-allelic recombination; human somatic cells.

INTRODUCTION

Chromosomal double-strand breaks (DSBs), either aris- ing spontaneously or induced by ionizing radiation, are particularly dangerous lesions, and their repair is important for maintaining the genomic integrity of all organisms [Van Dyck et al., 1999]. The failure to repair DSBs or their inaccurate repair may be mutagenic or lethal to cells, and can cause genetic defects that lead to genetic diseases and cancers [Khanna and Jackson, 2001; van Gent et al., 2001]. DSBs are usually repaired through either end-joining (EJ) or homologous recombination (HR) [Haber, 2000; Jackson, 2002]. EJ joins sequences at the broken ends with little or no homology in a nonconservative manner and, as a result, some genetic information is lost. HR, in contrast, requires extensive tracts of sequence homology and is basically a conservative repair pathway. HR can occur by gene con- version with or without crossing-over [Giver and Grosovsky, 1997; Cromie et al., 2001]. Non-crossing-over only involves the localized DNA region surrounding the DSB, whereas crossing-over results in a switch of the link- age relationships of all alleles from the break point to the

telomere. The repair of DSBs has been studied extensively in the yeast *Saccharomyces cerevisiae* [Paques and Haber, 1999]. HR is the primary pathway for repairing DSBs in yeast and almost always results in gene conversion without crossing-over [Haber, 1995]. This is in striking contrast to mammalian cells, where EJ is thought to be the predominant mechanism for repairing DSBs [Jackson and Jeggo, 1995]. However, the relative contribution of the two pathways and

their interaction in mammalian cells has not been firmly established.

In the study of DSB repair in mammalian cells, we employed the TK6 human lymphoblastoid cell line that is heterozygous for the thymidine kinase (*TK*) gene on chromosome 17q [Honma et al., 1997a,b, 2000]. The *TK*-gene mutation assay using the TK6 cells was first developed by Liber and Thilly [1982]. It can detect not only intragenic point mutations, but also loss of the functional allele (loss of heterozygosity [LOH]), which is considered a consequence of the repair of chromosomal DSBs. For repair of a DSB in the functional *TK* allele, HR produces homozygosity of the nonfunctional *TK* allele, while EJ brings about deletion in the functional *TK* allele, leading to its hemizygosity [Honma et al., 1997b]. We have demonstrated that homozygous LOH is the predominant spontaneous event, whereas hemizygous LOH is induced by ionizing irradiation, implying that HR repairs infrequently occurring DSBs, maintaining genomic integrity, whereas EJ repairs extensive DNA damage, enabling cell survival [Honma et al., 1997a; Jackson, 2002]. The mutational spectrum in the *TK* gene induced by nontargeting mutagenesis, however, has a strong bias for the recovery of HR mutants with crossing-over [Quintana et al., 2001]. DSBs generated within the *TK* gene can be recovered by any repair pathway as TK-deficient mutants. HR mutants with crossing-over, however, frequently result from the repair of DSBs outside the *TK* gene, which cannot be recovered by EJ and HR without crossing-over, because such genetic events are localized and do not affect the *TK* gene. Thus, the mutational spectrum for nontargeted mutagenesis does not provide appropriate information to elucidate the relative contribution of each DSB repair pathway.

Recently, an understanding of mammalian EJ and HR has emerged from systems that use the rare cutting restriction endonuclease I-*Sce*I from *Saccharomyces cerevisiae* [Johnson and Jasin, 2001]. Because the 18-bp recognition sequence of I-*Sce*I is infrequent enough to be naturally absent from most genomes, and can be introduced into a chromosome by transfection, it is possible to generate site-specific DSBs in a mammalian chromosome by expressing the enzyme in the genetically modified cells. Using this unique system, it has been demonstrated that DSBs in mammalian chromosomes initiate HR as well as EJ, and that deficiency or overexpression of *Rad51* and its paralogues, which have a central role in HR, can influence the efficiency of HR [Rijkers et al., 1998; Cui et al., 1999; Takata et al., 2001]. These systems, however, have used artificial reporter substrates based on exogenous drug-resistance genes and are biased in favor of detecting specific deletion and recombination events [Taghian and Nickoloff, 1997; Sargent et al., 1997; Liang et al., 1998; Lin et al., 1999]. Most of these models, in particular, cannot detect inter-allelic recombination, which is expected to be a major HR pathway for repairing chromosomal DSBs in mammalian cells. Moynahan and Jasin [1997] engineered a recombinational substrate

containing an I-*Sce*I site integrated into the retinoblastoma (*Rb*) gene of mouse embryonic stem cells and demonstrated a significant contribution of inter-allelic recombination for repairing DSBs, but the contribution of EJ was not clear. Thus, the previous DSB studies using the I-*Sce*I system have been useful for elucidating the molecular mechanisms of the repair pathways, but do not provide a general model for demonstrating the fate of a DSB in mammalian cells.

In the present study, we developed a system to trace the fate of DSBs that occur in a single-copy human gene. We introduced an I-*Sce*I site into the endogenous *TK* gene of TK6 cells by gene targeting. Unlike nontargeted mutagenesis, this system makes it possible to recover efficiently cell clones resulting from the repair of DSBs at a defined site. Using this system, we evaluated the relative contribution of EJ and HR for repairing DSBs and investigated the genetic consequences of each pathway at the molecular and cytogenetic level. This is the first report tracing the fate of a DSB occurring in an endogenous single-copy gene in the human genome.

MATERIALS AND METHODS

Vectors

The first targeting vector, pTK4, was designed to disrupt exon 5 of the *TK* gene by replacement with a *neo* gene. It was constructed as follows: (1) a region containing exons 6 and 7 of the *TK* gene (position 12,002–13,367) was amplified by a polymerase chain reaction (PCR) in which a *Xba*I linker was added to the 5′-primer. The amplified product was cleaved by *Xba*I and *Bam*HI and was cloned into pBluescript II (Stratagene, La Jolla, CA); (2) a 1,637-bp *Ssp*I-*Eco*O109I DNA fragment containing a simian virus 40 (SV-40) early-promoter-driven *neo* gene was cleaved from pEGFP-C1 (BD Biosciences-Clontech, Tokyo, Japan), modified with a *Not*I linker, and then cloned into the above plasmid; and (3) a region containing the last part of intron 4 (position 9,291–11,850) was amplified using a 3′-primer modified with a *Sac*II linker. The PCR product was cleaved by *Sac*I and *Sac*II, and cloned into the above plasmid.

The second targeting vector, pTK10, consisted of about 6 kb of the original *TK* gene encompassing exons 5, 6, and 7, and an I-*Sce*I site, which was used to revert the *TK* gene disrupted by pTK4. To construct pTK10, a region containing exons 5, 6, and 7 (positions 7,248–13,367) was amplified using a 5′-primer modified with a *Xho*I linker. The PCR product was cleaved by *Xho*I and *Bam*HI, and cloned into pBluescript II. A 31-bp DNA fragment containing the 18-bp I-*Sce*I site was formed by annealing the two oligonucleotides (5′-gatccATTACCCTGTTATCCCTActctcgag-3′ and 5′-gatcctcgugagTAGGGATAACAGGGTAATg-3′), producing *Bgl*II compatible sites at both ends. The DNA fragment was inserted into the *Bgl*II site of the above plasmid.

The I-*Sce*I-expressing vector, pCMV3×nls-I-*Sce*I (kindly provided by Dr. J. Nickoloff, University of New Mexico School of Medicine, Albuquerque, NM), contains the I-*Sce*I-nuclease coding sequence fused at its 5′-end to a triplicate nuclear localization signal, driven by the CMV promoter, and terminated by the bovine growth hormone polyadenylation signal [Brenneman et al., 2002].

Cell Construction

TK6 human lymphoblastoid cells are heterozygous for a point mutation in exon 4 of the *TK* gene [Grosovsky et al., 1993]. They were grown in

RPMI 1640 medium (Gibco-Invitrogen, Carlsbad, CA), supplemented with 10% heat-inactivated horse serum (JRH Biosciences, Lenexa, KS). TK-deficient clones were generated by transfecting cells with the first targeting vector that had been linearized with ScaI. TK6 cells (2 × 10⁷) were suspended with 20 μg of the linearized vector DNA in 0.8 ml of serum-free RPMI 1640 medium, transferred into a 0.4-cm gap chamber, and electroporated with an electroporation unit (Bio-Rad, Hercules, CA) set at 950 μF and 250 V. After 72 hr, the cells were seeded into 96-well microwell plates in the presence of 2.0 μg/ml trifluorothymidine (TFT) and 500 μg/ml G418. TK-deficient clones were isolated 2 weeks later, as described previously [Honma et al., 1997a]. One of clones, TKp4-2, was found to have the desired disruption of the TK gene (Fig. 1a). To obtain TK-revertant clones with an I-SceI site in the TK gene, we transfected TKp4-2 cells (2 × 10⁷) with the linearized second targeting vector, using the same techniques used above, and isolated histone acetyltransferase (HAT) (200 μM hypoxanthine, 0.1 μM aminopterin, 17.5 μM thymidine)-resistant clones. One revertant clone, TSCE5, was identified and its molecular structure was confirmed by PCR analysis (Fig. 1a). The cell line TSCER2 was spontaneously generated as a TK-deficient clone from TSCE5. It had a point mutation (G→A transition) at the bp 23 of exon 5 in the TK allele containing the I-SceI site, resulting in a compound heterozygote (TK⁻ᐟ⁻) (Fig. 1a).

I-SceI Expression

A total of 1 × 10⁷ cells were transfected in serum-free RPMI 1640 medium by electroporation with 20 μg of uncut pCMV3xnls-I-SceI vector or without vector as a control. After 72 hr, the cells were seeded into 96-well microwell plates in the presence of TFT (for TSCE5) or HAT (for TSCER2). Drug-resistant colonies were counted 2 weeks later and independently expanded.

DNA and Cytogenetic Analysis

DNA extraction and PCR analysis for LOH analysis at polymorphic sites in the TK gene and microsatellite markers were performed as described [Honma et al., 2000]. PCR analyses at the I-SceI site were performed to amplify the following products with the specified primers: the short fragment (Fig. 1a,b). 164F (5'-TGGGAGAATTAAGAGTTACTCC-3') and 196R (5'-AGC TTCCACCCCAGCAGCAGCT-3'); and the long fragment (see Fig. 4a,b), 175F (5'-TCGCTTGGCAATAGTAGGAGCT-3') and 199R (5'-ACTCTGTCTGTGCCGAGTGTA-3'). Amplification was performed by denaturation at 94°C for 5 min, followed by 25 cycles of 94°C for 1 min, 57°C for 1 min, 72°C for 2 min, and extension at 72°C for 10 min. PCR products were analyzed using an Agilent 2100 Bioanalyzer (Agilent Technologies, Waldbronn, Germany) and sequenced with an ABI 310 genetic analyzer (Applied Biosystems, Foster City, CA).

Spectral karyotyping (SKY) was used for the cytogenetic analysis of some TK-deficient mutants. The procedure was performed according to the manufacturer's recommendations as previously described [Honma et al., 2002]. Metaphase images were captured and analyzed on a SKY vision cytogenetics workstation (Applied Spectral Imaging, Carlsbad, CA) attached to an Olympus model 50 fluorescence microscope. At least five metaphase cells were analyzed per slide.

RESULTS

Experimental Design

To investigate the fate of DSBs occurring in the human genome, we used human lymphoblastoid cells containing an I-SceI recognition site in the endogenous TK gene. Human lymphoblastoid TK6 cells are heterozygous (TK⁺ᐟ⁻) for a

point mutation in exon 4 of the TK gene, which is on chromosome 17q. We introduced an I-SceI sequence into intron 4 near exon 5 of the functional TK allele. We employed two steps for gene targeting to minimize sequence divergence between the alleles (Fig. 1a), because integrated exogenous DNA sequences reduce sequence homology between alleles and probably suppresses inter-allelic recombination [Elliott et al., 1998]. The functional TK allele was first disrupted by replacement with a neo gene, and then it was reverted by a second targeting vector, pTK10, consisting of 6 kb of the original TK gene including exons 5, 6, and 7 and containing an I-SceI site. One of the recombinants, TSCE5, had a 31-bp DNA fragment containing the 18-bp I-SceI site inserted 75 bp upstream of exon 5 (Fig. 1b). TSCE5 cells can grow in HAT medium, but not in TFT medium (HAT-resistant/TFT-sensitive; HATʳ/TFTˢ). We next isolated spontaneously generated TK-deficient mutants from TSCE5. One of the mutants, TSCER2, had a point mutation (G→A transition) at bp 23 of exon 5. TSCER2 is compound heterozygote (TK⁻ᐟ⁻) for the TK gene and is HATˢ/TFTʳ.

Figure 1c shows the strategy used for detecting EJ in TSCE5 cells and HR in TSCER2 cells. When a DSB at the I-SceI site is repaired by EJ, a TK-deficient deletion mutant is isolated as TFTʳ in TSCE5 cells. With HR repair, on the other hand, a TK-proficient revertant, which is generated by inter-allelic recombination, is selected by HAT in TSCER2 cells. Theoretically, TSCE5 cells can also detect HR, if HR with crossing-over or long tract gene conversion makes the point mutation in exon 4 homozygous (TK⁻ᐟ⁻). We can, however, distinguish these events by further molecular analysis. Because both cell lines are identical except for their TK status and because the DSB occurs at the same position in both cell lines, this system can evaluate the contribution of EJ and HR without bias when the experiments are conducted simultaneously in both cell lines using the same conditions.

Almost All Chromosomal DSBs Were Repaired by EJ, But Not by HR

We transfected an I-SceI expression vector, pCMV3xnls-I-SceI, into TSCE5 cells by electroporation. TK-deficient mutant cells appeared at an average frequency of 274 × 10⁻⁶, more than 130-fold higher than in nontransfected cells (Fig. 2a). Because the transfection of the expression vector did not affect the mutant frequencies for the HPRT gene in TSCE5 cells and the TK gene in the original TK6 cells, the increase in mutant frequency must have been due to repair of DSBs at the I-SceI site (Fig. 2a). When TSCER2 cells were transfected with the I-SceI expression vector under the same conditions, TK-proficient revertants were isolated at an average frequency of 1.07 × 10⁻⁶, more than 200-fold higher than spontaneously occurring events (Fig. 2b). This strongly suggests that inter-allelic HR is also
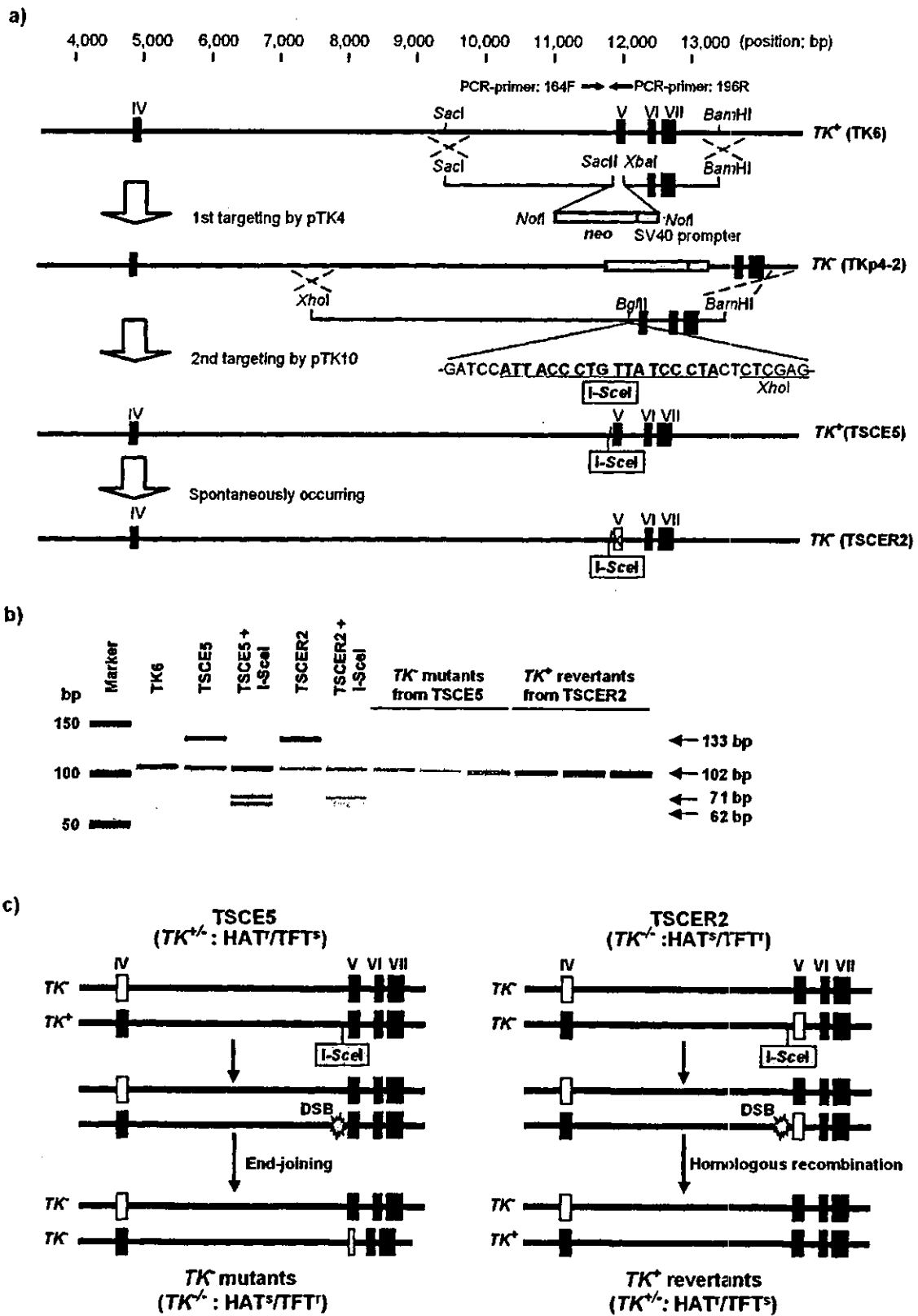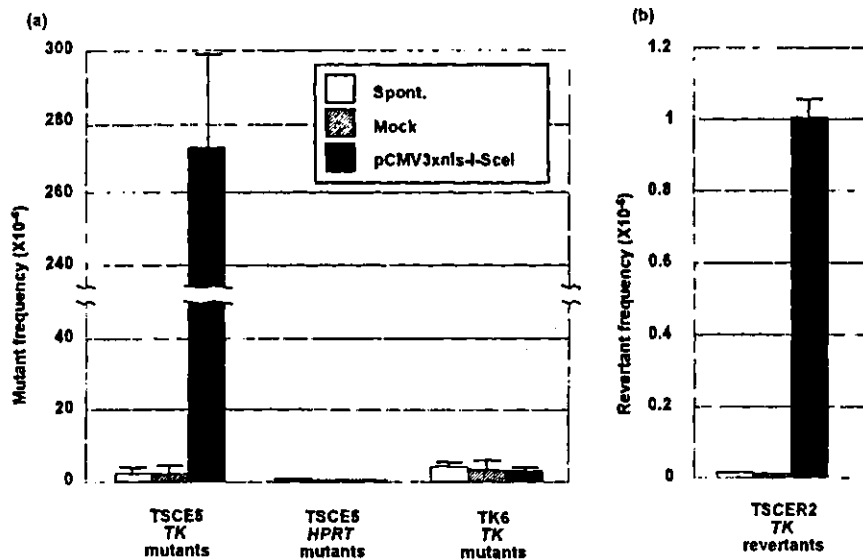
a)

b)

c)

Figure 1.

(a)

(b)

Fig. 2. Double-strand breaks (DSBs) induce both end-joining (EJ) and homologous recombination (HR). a: Transfection of TSCE5 cells with the I-Scel expression vector increases the thymidine kinase (TK)-deficient mutant frequency more than 130-fold compared with the control. No transfection-induced mutant induction was observed for the HPRT gene in TSCE5 cells and the TK locus in TK6 cells. b: Transfection of TSCER2 cells also increases the TK-proficient revertant frequency more than 200-fold compared with the control.

induced by a DSB. However, the fraction of HR was estimated to be much less than that of EJ, indicating that almost all DSBs were repaired by EJ.

EJ Mainly Caused Simple Deletions, But Also Produced Complicated DNA Rearrangements

We examined 44 TK-deficient mutants from TSCE5 cells at the molecular level. Every mutant lost the I-Scel site (Fig. 1b) by deletion and were hemizygous for the nonfunctional allele, suggesting that every mutant was generated by EJ. To obtain a rough determination of the extent of the deletion,

Fig. 1 (Overleaf). Creating assay systems to detect end-joining (EJ) and homologous recombination (HR) for repair of a double-strand break (DSB) at a I-Scel site in the human thymidine kinase (TK) gene. a: Structure of the functional TK allele in TK6 cells, and construction of the targeting vectors. The functional allele of the TSCE5 cell line is modified with a 31-bp DNA insert, including the 18-bp I-Scel site at a BglII site 75 bp upstream of exon 5. The TSCER2 cell line contains an additional point mutation (X) in exon 5 of the targeted allele, which results in an inactive the TK gene. b: PCR analysis of a DNA fragment with 164F and 196R primers. Because of the inserted DNA, the DNA from the TSCE5 cell line produces a 131-bp DNA fragment in addition to the original 100-bp fragment, and the larger product can be cleaved by I-Scel endnuclease. c: Schematic representation of the experimental system. Closed and open rectangles represent the wild-type and mutant exons of the TK gene, respectively. When a DSB at the I-Scel site is repaired by EJ, and it causes deletion in exon 5, TK-deficient mutants are isolated from TSCE5 cells in TFT medium. When HR repairs the DSB, TK-proficient revertants are generated from TSCER2 cells under HAT selection.
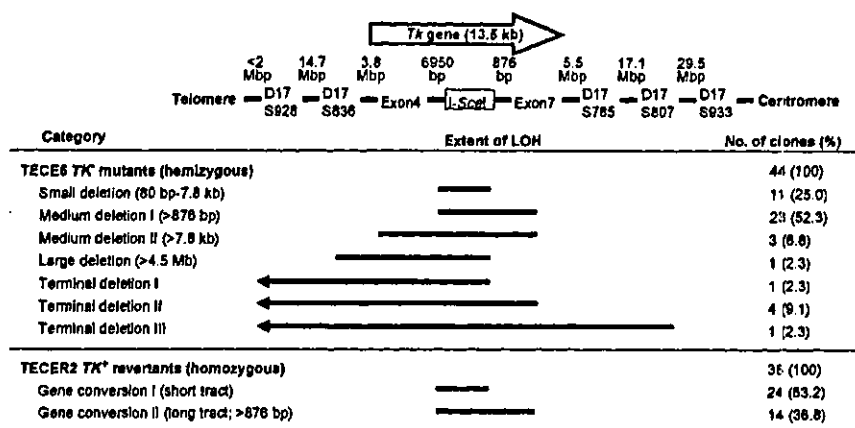
we analyzed LOH at polymorphic sites within the TK gene and at 5 polymorphic microsatellite loci surrounding the TK gene. The 13.5-kb human TK gene is located on chromosome 17q23.2. The TK gene in TSCE5 and TSCER2 cells has frame-shift dimorphisms in exons 4 and exon 7, which are 6,950 and 876 bp, respectively, from the I-Scel site. The 1-bp difference in the PCR products from these regions facilitated the LOH analysis [Honma et al., 2000]. Eleven (25%) of the mutants had small deletions not extending to either poymorphic site, and 26 (59%) showed medium-size deletions involving only the exon 4 and/or 7 polymorphic site in the TK gene. The remaining 7 mutants (16%) were the result of large interstitial or terminal deletions (Fig. 3).

We further analyzed small and medium deletions by PCR and direct sequencing to determine the exact size of deletions and the junction sequences generated by EJ. Eleven small and 23 medium deletion 1 mutants identified by LOH analysis were subjected to PCR using primers 175F and 199R, which amplified 5,618 bp (I-Scel allele) and 5,587 bp (non-I-Scel allele) products using DNA from TSCE5 cells (Fig. 4a,b). Twenty-two of the 34 mutants exhibited shorter PCR products of various sizes in addition to the original product in the gel analysis, whereas the other 12 mutants did not clearly show shorter products (Fig. 4a). Sequence analysis of the 22 shorter PCR products showed that 16 mutants resulted from simple deletions ranging from 109 to 3,964 bp. Zero to 6-bp microhomology was observed at the junctions in these mutants, indicating that a nonhomologous end-joining (NHEJ) model could explain the deletions

Fig. 3. Extent of (loss of heterozygosity (LOH) in thymidine kinase (TK)-deficient mutants from TSCE5 and TK-proficient revertants from TSCER2. Two frame-shift mutations in exons 4 and 7 of the TK gene and 5 microsatellite loci on chromosome 17q that are heteromorphic in the cell lines were used for the analysis. The human TK gene consists of 13.5 kb and maps to 17q23.2, oriented from telomere to centromere. The length of bars indicates the extent of LOH. Forty-four TSCE5 mutants and 36 TSCER2 revertants were analyzed.
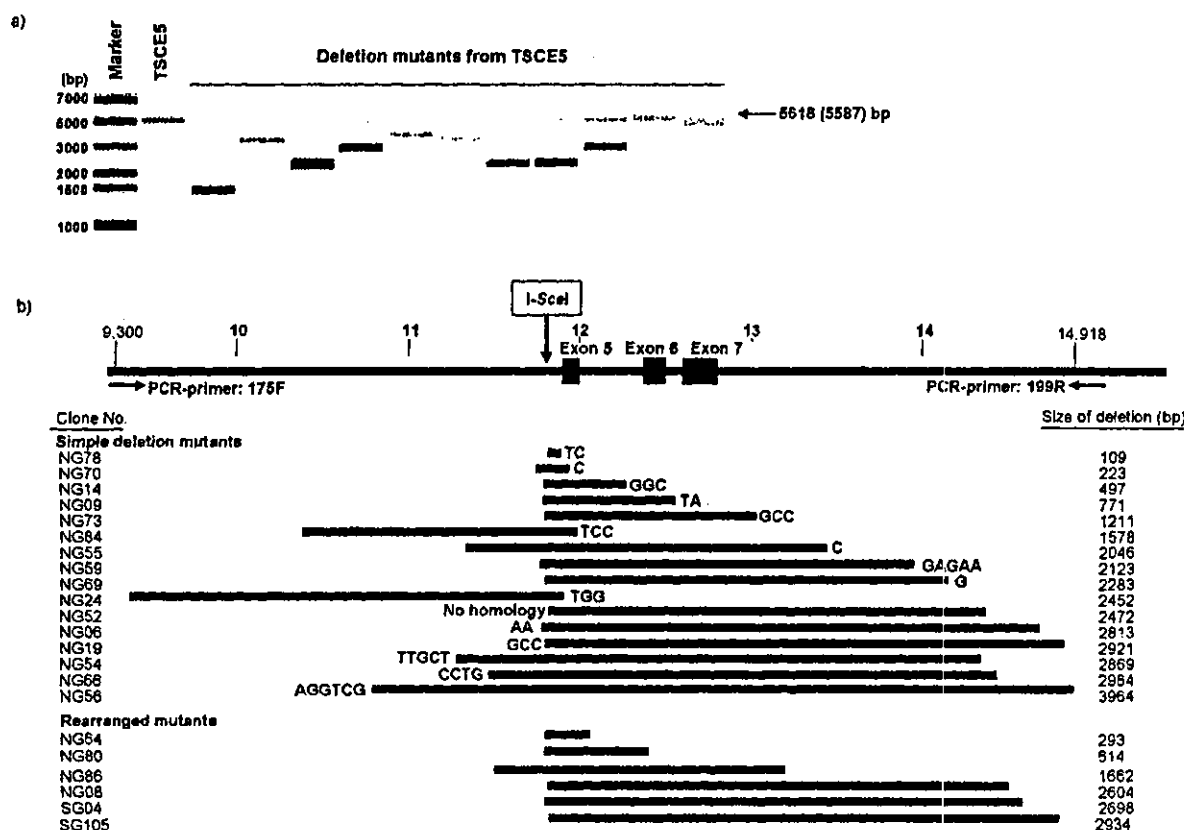

Fig. 4. Polymerase chain reaction (PCR) and sequence analysis of the regions flanking the I-SceI site in small deletion and medium deletion-I mutants (Fig. 3.) from TSCE5 cells. a: PCR analysis of a DNA fragment involving exons 5, 6, and 7 of the thymidine kinase (TK) gene with primers 175F and 199R. The DNA from the TSCE5 cell line produces 5,587-bp and 5,618-bp DNA fragments. DNAs from TK-deficient TSCE5 mutants ex-hibit shorter DNA fragments caused by deletion. b: Twenty-two of 34 mutants contained shorter PCR products. The length of bars indicates the extent of deletion. Sixteen mutants exhibited simple deletions with micro-homology sequences, which are indicated on the side of bars, and the other six mutants had deletions combined with complicated DNA rearrange-ments (Fig. 5).